

## COLLECTIVE FLOW IN NUCLEAR FRAGMENTATION INDUCED BY 4.4 GeV DEUTERON ON GOLD TARGET

V. A. Karnaukhov<sup>a</sup>, S. P. Avdeyev<sup>a</sup>, H. Oeschler<sup>b</sup>, V. V. Kirakosyan<sup>a</sup>,  
P. A. Rukoyatkin<sup>a</sup>, A. Budzanowski<sup>c</sup>, W. Karcz<sup>c</sup>, E. Norbeck<sup>d</sup>, A. S. Botvina<sup>e</sup>

<sup>a</sup> Joint Institute for Nuclear Research, Dubna

<sup>b</sup> Institut für Kernphysik, Darmstadt University of Technology, Darmstadt, Germany

<sup>c</sup> H. Niewodniczanski Institute of Nuclear Physics, Cracow, Poland

<sup>d</sup> University of Iowa, Iowa City, IA, USA

<sup>e</sup> GSI, Darmstadt, Germany

Nuclear multifragmentation in  $d(4.4 \text{ GeV}) + \text{Au}$  collision was studied with the  $4\pi$  setup FASA installed at the external beam of the Dubna Nuclotron. Data obtained are analyzed within the statistical model of multifragmentation. It is found that the kinetic energy spectra of intermediate mass fragments deviate from the predicted ones. It is explained by the collective flow caused by the thermal expansion of fragmenting nucleus.

Исследование ядерной мультифрагментации для взаимодействия  $d(4,4 \text{ ГэВ}) + \text{Au}$  проводилось на выведенном пучке нуклотрона в Дубне на  $4\pi$ -установке ФАЗА. Полученные данные проанализированы в рамках статистической модели мультифрагментации. Установлено, что спектры кинетической энергии фрагментов промежуточной массы отличаются от расчетных. Полученное отличие в спектрах объясняется коллективным потоком теплового расширения фрагментирующихся ядер.

PACS: 25.70.Pq; 24.10.Lx; 24.10.Pa; 25.55.-e

### INTRODUCTION

The process of multifragmentation is copious emission of intermediate mass fragments (IMF), which are heavier than  $\alpha$  particles, but lighter than fission fragments. Multifragmentation is the main decay mode of very excited nuclei ( $E^* \geq 4 \text{ MeV/nucleon}$ ). An effective way to produce hot nuclei is reactions induced by relativistic light ions. In this case, fragments are emitted by only one source — the slowly moving target spectator. Its excitation energy is almost entirely thermal. Therefore, light relativistic projectiles provide a unique opportunity for investigation of *thermal multifragmentation*.

It has been found experimentally for  $p(8.1 \text{ GeV}) + \text{Au}$  collisions that the process is characterized by two volumes of the fragmenting nucleus [1, 2]. One,  $V_t$ , corresponds to the chemical freeze-out state (on the top of the fragmentation barrier), when pre-fragments are formed. The fragment charge distribution drastically depends on  $V_t$ , and its value is estimated by comparison of the measured distribution with the model-calculated one:  $V_t = (2.6 \pm 0.2)V_0$ .

The other volume is reached by the nucleus after its descent from the top of the fragmentation barrier to the multiscission point. It is called the kinetic freeze-out volume,  $V_f$ . It was estimated via comparison of the kinetic energy spectra of the fragments with the calculated ones:  $V_f = (5.0 \pm 0.5)V_0$ . In both cases the statistical model of multifragmentation (SMM) was used [3, 4]. This model allowed the main properties of thermal multifragmentation to be successfully described.

This paper reports some new experimental data on thermal multifragmentation, which were obtained by the FASA collaboration for the collisions of 4.4 GeV deuterons with a gold target. The accumulated high statistics allows search for the deviation of the data from the SMM predictions.

## EXPERIMENTAL

The experiment has been performed with the  $4\pi$  setup FASA [5, 6] installed at the external beam of the Dubna superconducting accelerator Nuclotron. The FASA device consists of two main parts. One is the array of thirty  $dE$ - $E$  telescopes which serve as triggers for the readout of the FASA detectors. These telescopes allow measuring the fragment charge and energy distributions. The total solid angle of the telescopes is 0.3 sr. The other part is the fragment multiplicity detector (FMD) composed of 58 thin CsI(Tl) counters ( $30$ – $40$  mg/cm<sup>2</sup>), which cover 81% of  $4\pi$ . The FMD gives the number of IMFs in the event and their spatial distribution.

Each fragment telescope consists of a compact ionization chamber used as the  $dE$  counter and a Si(Au) semiconductor detector used as the  $E$  spectrometer. Effective thickness of the  $E$  detector is around  $700$   $\mu$ , which is enough to measure the energy spectra of all intermediate mass fragments. The ionization chamber has the shape of a cylinder (50 mm in diameter, 40 mm high). It is made from polished brass. The entrance and exit windows are made from organic films ( $\sim 100$   $\mu$ g/cm<sup>2</sup>) covered with a thin gold layer prepared by thermal evaporation. Gold wire of 0.5 mm in diameter is used as an anode. The working gas is CF<sub>4</sub> at a pressure of 50 Torr.

A self-supporting Au target ( $\sim 1.5$  mg/cm<sup>2</sup>) is located at the center of the FASA vacuum chamber. The target is supported by thin tungsten wires at 45°. The energy calibration of the counters was done periodically using a precise pulse generator and a <sup>241</sup>Am alpha source. The calibrating procedure was performed with the beam switched off, when the target was replaced by the calibrating source by means of a special mechanical system. The beam intensity was around  $10^{10}$  particles per spill. The beam spot was continuously controlled by two multiwire proportional chambers placed at the entrance and exit of the FASA device. The beam intensity was measured by the ionization chamber located 150 cm behind the target. The spill length was 1.5 s, the frequency of the beam bursts was 0.1 Hz.

## EXPERIMENTAL RESULTS

The events of fragmentation are detected as coincidence of  $dE$  and  $E$  signals. Figure 1 gives an example of the  $dE$ - $E$  plot measured by one of the telescopes for  $d + \text{Au}$  collisions at 4.4 GeV. The fragment energy is given at the front of the telescope. It is obtained from the measured value by adding the energy lost on the way from the target to the  $E$  detector.

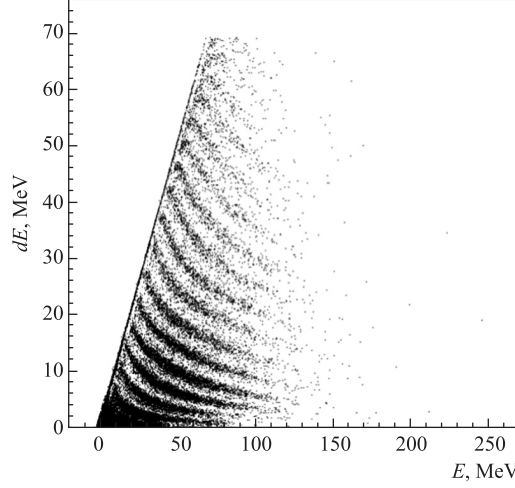


Fig. 1. Multifragmentation in  $d(4.4 \text{ GeV}) + \text{Au}$  collisions, the  $dE-E$  plot measured by one of the thirty FASA telescopes, the total number of events detected is around  $1.5 \cdot 10^4$

The loci for different intermediate mass fragments are well resolved in the range from lithium ( $Z = 3$ ) to sulfur ( $Z = 16$ ). The energy cutoff caused by adsorption of the low energy fragments before the Si(Au) detector increases with  $Z$  of fragments. Thus, Ne fragments with the energy less than 25 MeV do not reach the  $E$  counter.

The energy spectra of intermediate mass fragments with a given charge may be obtained without any significant admixture. Figures 2–4 show the kinetic energy spectra for some selected fragments between  ${}^4\text{Be}$  and  ${}^{14}\text{Si}$ . Note that transverse energy is given,  $E_t = E \sin^2 \theta$ ,

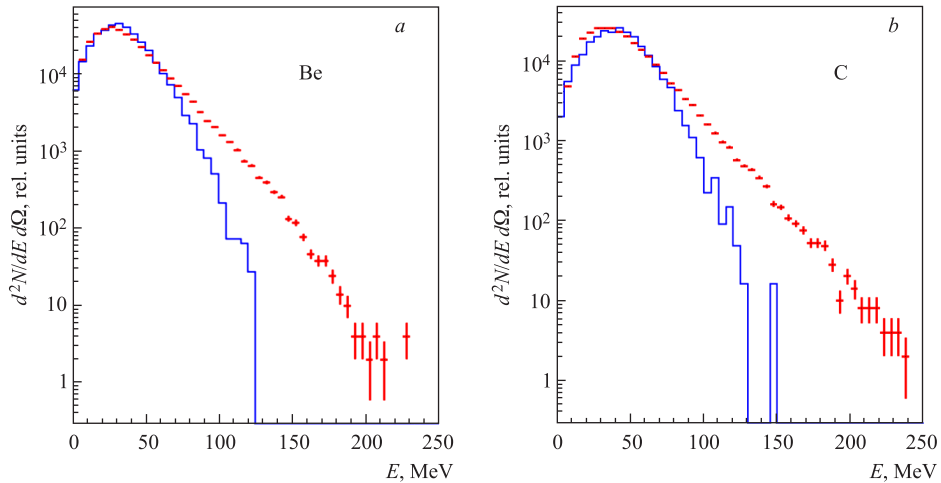


Fig. 2. Kinetic energy spectra of Be (a) and C (b) produced in  $d(4.4 \text{ GeV}) + \text{Au}$  collisions. Lines are calculated within the combined INC + Exp + SMM model

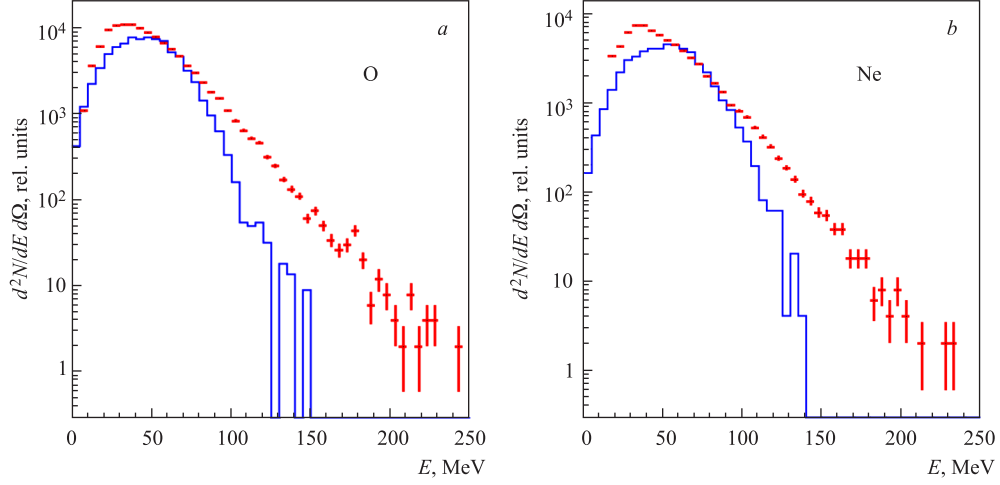


Fig. 3. Kinetic energy spectra of oxygen (a) and neon (b) produced in  $d(4.4 \text{ GeV}) + \text{Au}$  collisions, lines are calculated within the INC + Exp + SMM approach

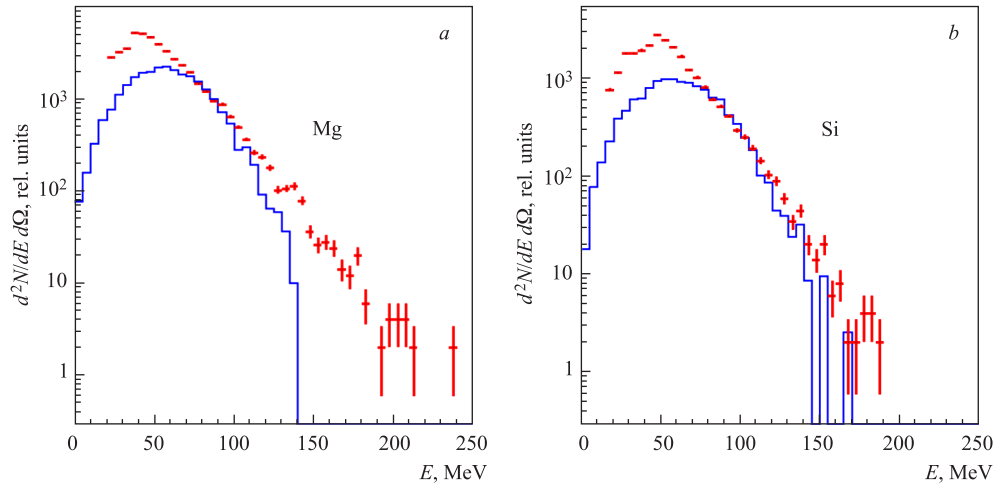


Fig. 4. Kinetic energy spectra of fragments with  $Z = 12$  and  $14$ , lines are calculated within the combined INC + Exp + SMM model

where  $\theta$  is the polar angle of fragment detection. It is done to diminish the influence of the source velocity. The spectra are composed by summing those measured by all the telescopes of the FASA setup.

The lines are obtained within the combined INC + Exp + SMM model [7]. The first step of the reaction is described by the intranuclear cascade calculations [8]. The expansion of the excited residuals accompanied by additional loss of mass and energy is taken into account by some empirical procedure (Exp). The statistical multifragmentation model [4] followed by the multibody Coulomb trajectory [9] describes the final step of the collision. The model spectra

are close to the data in the vicinity of the maxima for the lighter fragments considered, but the calculations underestimate the yield for the high energy tail. The inverse slope parameter here is larger than the predicted one. This deviation diminishes with increasing fragment charge.

## DISCUSSION

The model predicted spectra obtained by the multibody Coulomb trajectory calculation [10]. The main part of the fragment kinetic energy ( $E_c$ ) is originated in the Coulomb expansion of the system after the breakup of the hot nucleus. The observed deviation of the kinetic energy spectra may be attributed to the radial flow generated by thermal pressure,  $P_T$ , in the fragment source. In this connection one should remember the papers by W. Friedman who first considered the nuclear expansion driven by heating [11, 12]. In the following the flow problem was studied in detail by W. Reisdorf and FOPI collaboration at GSI [13, 14].

According to [13], pressure is directly related to thermal energy per nucleon  $W_T$ :

$$P_T = \alpha \rho W_T. \quad (1)$$

The coefficient  $\alpha$  is equal to  $2/3$  for the nonrelativistic Fermi gas;  $\rho$  is the nuclear density;  $W_T$  is the thermal energy per nucleon related to the nuclear temperature  $T$

$$W_T = \frac{\pi^2}{4\varepsilon_F} T^2 \left( \frac{\rho_0}{\rho} \right)^{2/3}. \quad (2)$$

Thus, the final fragment velocity is the sum of the «Coulomb» and «flow» velocities:  $v = v_c + v_{\text{flow}}$ . This effect is not taken into account in the statistical model SMM. Fragment energy per nucleon becomes

$$E \approx E_c \left( 1 + 2 \frac{v_{\text{flow}}}{v_c} \right), \quad (3)$$

$$E - E_c = 2E_c \frac{v_{\text{flow}}}{v_c}. \quad (4)$$

According to Eq. (4), the shift of  $E$  in relation to  $E_c$  is proportional to  $E_c$ . This results in the increase of the inverse slope parameter of the spectrum tails as observed. The flow velocity can be estimated from Eq. (4). For the Be fragment with energy between 130 and 170 MeV the flow velocity is  $\sim 1/3$  of the predicted one ( $v_c$ ).

The flow velocity is assumed to be a linear function of the scaled radius  $r/R$ , where  $R$  is the time-dependent outer radius of the expanding system and  $r$  is the radial coordinate of the detected fragment:  $v_{\text{flow}}(Z) = v_{\text{flow}}^0 r/R$ . The velocity on the surface of the emitting nucleus is designated as  $v_{\text{flow}}^0$ . The total flow energy can be estimated by integrating the nucleon flow over the available volume at freeze-out. For a uniform system with  $A$  nucleons, one gets the following equation for the flow energy [15]:

$$E_{\text{flow}}^{\text{tot}} = \frac{3}{10} A m_N (v_{\text{flow}}^0)^2 \left( 1 - \frac{r_0}{R} \right)^5, \quad (5)$$

where  $m_N$  and  $r_0$  are the nucleon mass and radius. The calculation with Eq. (5) gives 50–60 MeV for the flow energy. This estimation was done with the use of the data for Be

fragments. Note that this value is  $\sim 10\%$  of the thermal part of the excitation energy of the fragmenting nucleus [16]. As the mass of fragment increases the mean value of its radial coordinate becomes smaller. This is the reason for diminishing the radial flow for heavier fragments.

The authors are grateful to the staff of the Dubna Nuclotron for supplying the beam to perform this study. We are indebted to V. D. Kekelidze and A. G. Olchevski for their support. This research was supported in part by the Russian Foundation for Basic Research, project No. 10-02-01002a and by the Grant of the Polish Plenipotentiary to JINR.

#### REFERENCES

1. *Karnaikhov V. A. et al.* // *Phys. Rev. C.* 2004. V. 70. P. 041601(R).
2. *Karnaikhov V. A. et al.* // *Nucl. Phys. A.* 2005. V. 749. P. 65c.
3. *Botvina A. S. et al.* // *Yad. Fiz.* 1985. V. 42. P. 1127.
4. *Bondorf J. et al.* // *Phys. Rep.* 1995. V. 257. P. 133.
5. *Avdeyev S. P. et al.* // *Nucl. Instr. Meth. A.* 1993. V. 332. P. 149.
6. *Kirakosyan V. V. et al.* // *Instr. Exp. Techn.* 2008. V. 51, No. 2. P. 159.
7. *Avdeyev S. P. et al.* // *Nucl. Phys. A.* 2002. V. 709. P. 392.
8. *Toneev V. D. et al.* // *Nucl. Phys. A.* 1990. V. 519. P. 463c.
9. *Akishin P. G. et al.* // *Comp. Math. Appl.* 1997. V. 34, No. 2–4. P. 45.
10. *Shmakov S. Yu. et al.* // *Phys. At. Nucl.* 1995. V. 58. P. 1635.
11. *Friedman W. A.* // *Phys. Rev. Lett.* 1998. V. 60, No. 21. P. 2125.
12. *Friedman W. A.* // *Phys. Rev.* 1990. V. 42, No. 2. P. 667.
13. *Reisdorf W., Ritter H. G.* // *Ann. Rev. Nucl. Part. Sci.* 1997. V. 47. P. 663.
14. *Reisdorf W. et al.* // *Nucl. Phys. A.* 1997. V. 612. P. 493.
15. *Karnaikhov V. A. et al.* // *Phys. At. Nucl.* 2003. V. 66. P. 1242.
16. *Avdeyev S. P. et al.* // *Phys. Lett. B.* 2001. V. 503. P. 256.

Received on May 13, 2010.